Published in final edited form as:
Free Radic Biol Med. 2008 September 15; 45(6): 866–874. doi:10.1016/j.freeradbiomed.2008.06.023.

Involvement of inducible nitric oxide synthase in hydroxyl radical-mediated lipid peroxidation in streptozotocin-induced diabetes

Krisztian Stadler[*,#,&], **Marcelo G. Bonini**[#,&], **Shannon Dallas**[&], **JinJie Jiang**[&], **Rafael Radi**[$], **Ronald P. Mason**[&], and **Maria B. Kadiiska**[&]

&Laboratory of Pharmacology and Chemistry, National Institute of Environmental Health Sciences, National Institutes of Health, P.O. Box 12233 MD F0-02, Research Triangle Park, NC 27709

$*Departamento de Bioquímica, Facultad de Medicina, Universidad de la República, Avda. Gral. Flores 2125, 11800 Montevideo, Uruguay.*

Abstract

Free radical production is implicated in the pathogenesis of *diabetes mellitus*, where several pathways and different mechanisms were suggested in the pathophysiology of the complications. In this study, we used electron paramagnetic resonance (EPR) spectroscopy combined with *in vivo* spin-trapping techniques to investigate the sources and mechanisms of free radical formation in streptozotocin-induced diabetic rats. Free radical production was directly detected in the diabetic bile, which correlated with lipid peroxidation in the liver and kidney. EPR spectra showed the trapping of a lipid-derived radical. Such radicals were demonstrated to be induced by hydroxyl radical through isotope labeling experiments. Multiple enzymes and metabolic pathways were examined as the potential source of the hydroxyl radicals using specific inhibitors. Neither xanthine oxidase, cytochrome P450s, the Fenton reaction, nor macrophage activation were required for the production of radical adducts. Interestingly, inducible nitric oxide synthase (apparently uncoupled) was identified as the major source of radical generation. The specific iNOS inhibitor 1400W as well as L-arginine pretreatment reduced the EPR signals to baseline levels, implicating peroxynitrite as the source of hydroxyl radical production. Applying immunological techniques, we localized iNOS overexpression in the liver and kidney of diabetic animals, which was closely correlated with the lipid radical generation and 4-hydroxynonenal-adducted protein formation, indicating lipid peroxidation. In addition, protein oxidation to protein free radicals occurred in the diabetic target organs. Taken together, our studies support inducible nitric oxide synthase as a significant source of EPR-detectable reactive intermediates, which leads to lipid peroxidation and may contribute to disease progression as well.

Introduction

Despite the fact that *diabetes mellitus* is one of the best characterized chronic metabolic diseases, it is still a major concern in human health and shows increasing incidence. According to a World Health Organization study, the estimated number of patients with diabetes

To whom correspondence should be addressed. Laboratory of Pharmacology and Chemistry, National Institute of Environmental Health Sciences, National Institutes of Health, P.O. Box 12233 MD F0-02, Research Triangle Park, NC 27709. Tel:919-541-3381, Fax: 919-541-1043, email: stadlerk@niehs.nih.gov.
[#]These authors contributed equally to this work.

worldwide is around 170 million and projected to reach about 300 million in 2025 [1;2]. As a consequence, this will lead to an increased number of people with diabetic complications such as diabetic nephropathy, neuropathy, retinopathy and, last but not least, diabetic cardiovascular complications and atherosclerosis, which is the major cause of death resulting from the disease [3]. Several trial studies emphasize the importance of persistent hyperglycemia in the pathogenesis of diabetes [4;5]. It is present in both type 1 and type 2 diabetes and plays a key role in the development of complications through different and multiple mechanisms, including nonenzymatic glycation [6], protein kinase C activation [7], and increased aldose reductase activity [8;9]. There is accumulating evidence, especially in diabetic animal models (such as streptozotocin-diabetic rats and mice), that hyperglycemia induces oxidative stress, and reactive species such as lipid peroxides and glucose-derived aldehydes contribute to the pathogenesis of the disease and the development of complications as well [10–15]. Various studies propose different sites for production of reactive species in diabetes.

Under hyperglycemic conditions, the polyol pathway becomes activated; here aldose reductase plays a role [16], converting glucose to sorbitol and producing oxidative stress through superoxide radical anion formation. Obrosova and co-workers have studied the inhibition of aldose reductase, focusing on diabetic complications [17;18]. They also emphasized the possible role of peroxynitrite, nitration, and nitrotyrosine formation in certain diabetic complications such as neuropathy [19;20]. Mitochondria as a site of superoxide formation under hyperglycemia is one of the most widely studied areas in the etiology of diabetes. Hyperglycemia-induced overproduction of superoxide by the mitochondrial electron transport chain activates three major pathways of hyperglycemic damage in aortic endothelial cells by inhibiting GAPDH activity [21]. This investigation led to a unifying mechanism in the field of diabetic pathophysiology, alterations of several metabolic pathways, and mitochondrial oxidative stress [22].

Other studies have focused on the possible role of NOS enzymes in the disease. If these enzymes are affected, under oxidative stress conditions they may fail to produce NO or may produce both NO and superoxide, which is likely to result in peroxynitrite formation and contribute to the complications. Uncoupling of endothelial NOS (eNOS) by peroxynitrite has been shown previously [23;24]. This may be an additional mechanism by which glucose contributes to endothelial dysfunction in diabetes. Regulation of eNOS transcription by reactive species produced in hyperglycemia has also been suggested [25]. There are a few attempts to prove free radical formation in any of the diabetic models directly and thus offer mechanisms through which these species could affect the tissue environment as the disease progresses. One study used direct spin-trapping methods to show that free radical formation occurs in the pancreatic islets upon addition of exogenous cytokines [26]. Other studies have been performed to demonstrate the possibility of radical generation in a whole diabetic animal [27;28] through L-band EPR spectroscopy which used non-specific spin probes.

Here we provide EPR data for *in vivo* free radical formation as a mechanism that occurs in STZ-induced diabetes and contributes to lipid peroxidation and protein nitration in the liver and kidney. STZ-induced diabetes is associated with signs of fatty liver [29] and was found to show nephropathic changes and kidney damage as well [30]. We have addressed these questions through the combined use of *in vivo* EPR methodologies and spin trapping to specifically detect increased free radical production in the diabetic rat liver. In addition, a detailed search for the sources of reactive intermediates was conducted through the combination of EPR and immunological techniques. The uniqueness of EPR spectroscopy combined with *in vivo* spin trapping and isotope labeling allowed us to identitify iNOS as a source of hydroxyl radicals in diabetes. Furthermore, our studies indicate that iNOS protein expression was correlated with increased free radical production in the organs examined. The role of iNOS was further confirmed by EPR using a specific iNOS inhibitor, 1400W, and L-

arginine supplementation. Lipid and protein damage paralleled iNOS overexpression in the liver and kidney of diabetic animals as demonstrated by the immunohistochemical detection of 4-hydroxynonenal-adducted proteins resulting from increased lipid peroxidation. Protein nitration was also evidenced and colocalized with iNOS in the liver. Such results clearly link iNOS overexpression with increased free radical formation and lipid peroxidation in the disease, which might be involved in the progression of diabetes. iNOS-mediated free radical production in diabetes

Experimental procedures

Materials

α-(4-pyridyl-1-oxide)-*N*-*t*-butylnitrone (POBN) was obtained from Alexis Biochemicals (San Diego, CA). Streptozotocin (STZ), dimethylsulfoxide (DMSO), 2,2′-dipyridyl (DP), bathocuproinedisulfonic acid (BC), deferoxamine mesylate (Desferal), aminoguanidine, allopurinol, 1-aminobenzotriazol, gadolinium(III)-chloride ($GdCl_3$) and L-arginine were all obtained from Sigma (St.Louis, MO). ^{13}C-DMSO was obtained from Isotec. *N*-(3-aminomethyl)benzylacetamidine (1400W) was from Calbiochem-Novabiochem (La Jolla, CA). Paraformaldehyde and sucrose were from ICN (Orangeburg, NY). For the confocal and Western blot studies, monoclonal iNOS primary antibody was from Sigma (St.Louis, MO). Alexafluor 488 goat anti-mouse secondary antibody was from Invitrogen (Carlsbad, CA).

Animals

Sprague-Dawley male rats weighing 100–120 g (Charles River Breeding Laboratories) were used in all experiments. Rats were housed in a room with air conditioning and a 12/12 h light/dark cycle, fed a standard rat chow (NIH open formula, Ziegler Brothers, Gardner, PA) and had access to water *ad libitum*. Diabetes was induced by a single dose of streptozotocin (65 mg/kg, i.p., in 0.1 M citrate buffer, pH = 4.6) which is known to be excreted within 48 h from injection and therefore cannot be a direct cause of oxidative stress thereafter [31]. Development of the disease was confirmed three days later with a urinary glucose test strip (Chemstrip uGK, Roche). One month after the onset of the disease, animals were anesthetized by i.p. injection of Nembutal (50 mg/kg), the spin trap POBN was injected i.p. and bile was collected immediately by bile duct cannulation via a segment of PE-10 tubing (Becton Dickinson). For time course studies, similar experimental protocols were followed at one, two, or three weeks after streptozotocin injection. Blood was collected at the end of each experiment to verify the presence of diabetes by measuring blood glucose levels. Measurement of serum glucose, aspartate aminotransferase (AST), alanine aminotransferase (ALT), and triglycerides was performed at NIEHS by the Laboratory of Experimental Pathology. Rats with normal glucose levels were excluded from the study. Body weights and water consumption were also monitored throughout the experiments. All studies were approved by the institutional review board and adhered to NIH guidelines for the care and handling of experimental animals.

In vivo studies

POBN was dissolved in saline and administered i.p. at 1 g/kg body weight, and bile samples (approximately 300 μl) were collected every 30 min for 2.5 h into plastic Eppendorf tubes containing a 50 μl solution of bathocuproine disulfonic acid and 2,2’-dipyridyl (30 mM, respectively, to prevent *ex vivo* free radical production). Kidney tissue samples were also collected at the end of the spin-trapping experiments, and lipid extraction was performed using chloroform/methanol (2:1) as described previously [32]. Samples were frozen in dry ice immediately after collection and stored at −80°C until the EPR measurements.

During inhibitor studies, after a month of diabetes, diabetic rats were divided into several different groups and received different metabolic inhibitors before bile cannulation and spin

trapping. Each group contained at least 6 animals. In each set of experiments, DMSO (1 ml/kg body weight, i.p.) was injected simultaneously with POBN. In the experiments with isotope-labeled DMSO, ^{13}C-DMSO was administered i.p. (1 ml/kg body weight) instead of unlabeled DMSO. ABT (100 mg/kg, i.p.) [33] or Desferal (50 and 200 mg/kg, i.p.) [34] in saline was administered to rats 2 or 1 h before spin trapping, respectively. Allopurinol (100 mg/kg) was given i.p. 5 and 24 h before the POBN and DMSO injection [35]. $GdCl_3$ (10 mg/kg) was injected intravenously 24 h before the spin-trapping experiments [36]. Aminoguanidine (200 mg/kg) or 1400W (15 mg/kg) was administered 30 min or 1 h prior to spin trapping, respectively [37]. L-arginine (100 mg/kg) was administered 30 min prior to spin trapping.

Ex vivo studies

Control *ex vivo* studies were made by mixing POBN (20 mM) and DMSO (10 mM) in the collecting tube containing 30 mM bathocuproine disulfonic acid and 30 mM 2,2′-dipyridyl, and diabetic bile was collected into the solution. All *ex vivo* experiments were done in triplicate.

EPR studies

All EPR spectra were recorded at room temperature in a quartz flat cell on a Bruker EMX EPR spectrometer equipped with a super high-Q cavity (Bruker, Billerica, MA). Spectra were recorded using an IBM-compatible computer interfaced with the spectrometer with the following instrument settings and conditions: 20.2 mW microwave power, 100 kHz modulation frequency, 1.25 G modulation amplitude, 1,300 ms time constant, 655 ms conversion time and a single scan of 80 G. The simulations of EPR spectra and determination of hyperfine coupling constants were performed using the WINSIM program developed in our laboratory [38] and available on the internet for download at http://epr.niehs.nih.gov.

Confocal microscopy

For confocal studies, animals were divided into two groups, control and diabetic. After one month of diabetes, animals were anesthetized by i.p. injection of Nembutal (50 mg/kg), and liver perfusion was carried out through the *vena portae* using a peristaltic pump. First, saline was perfused through the liver for 10 min; then the system was switched to 3.5 % paraformaldehide solution in PBS (pH = 7.4) for *in situ* tissue fixation. After fixation, livers were removed and placed into 30 % sucrose for 24 h. Tissues were then sliced on a microtome into 70 μm sections and placed in PBS, then permeabilized with 0.1 % Surfact-Amps-X-100 for 1 h. After blocking with 0.1 % bovine serum albumin in PBS, staining of iNOS was performed using monoclonal anti-iNOS as the primary antibody and an Alexafluor 488 anti-mouse secondary. Nitrotyrosine staining was carried out using a rabbit polyclonal anti-nitrotyrosine antibody [39] and an Alexafluor 568 anti-rabbit secondary. Secondary controls were made to determine background fluorescence by omitting the primary antibody, but applying the secondary antibody. Slices were mounted on microscope cover glasses (22 × 22 mm, 1 ½ thickness) (Erie Scientific Co. Portsmouth, NH), and sections were observed under a confocal laser microscope (Zeiss).

Western blotting

Western blot analysis was used to determine iNOS protein expression in control and diabetic rat liver, kidneys and lungs after one month of diabetes, and at each timepoint as well. Tissue samples were homogenized with a Polytron homogenizer in RIPA buffer containing a mixture of protease inhibitors. After incubation at 4 °C for 30 min, samples were centrifuged at 14,000 rpm for 15 min. Protein concentrations were quantitated with a protein assay kit (Biorad), and an equal amount of protein (40 μg/lane) was separated on reducing NuPAGE 4–12 % Bis-Tris gel (Invitrogen) and transferred to a nitrocellulose membrane. After overnight blocking (1% bovine serum albumin, 1% amicase in PBS 0.1M, pH=7.4), the membrane was probed with a

monoclonal iNOS primary antibody (Sigma) followed by an anti-mouse secondary antibody and CDP-Star chemiluminescent substrate (Roche). Western blot band intensities were quantified using the Image J program (download available at http://rsb.info.nih.gov/ij/).

Immunohistochemistry

For the immunohistochemical detection of 4-hydroxynonenal protein adducts, control and diabetic liver, kidney and lung tissue slices were fixed in neutralized formaldehyde for 24 hours, then transferred into 70 % ethanol. Tissue samples were embedded into paraffin, and three micrometer sections were cut and mounted onto glass slides. Monoclonal anti-4-hydroxynonenal protein adduct antibody (Alexis Biochemicals, San Diego, CA) was applied as a primary antibody and anti-rabbit as the secondary to detect the adduct in tissue samples.

Statistical analysis

Data were expressed as mean ± SEM except for EPR hyperfine coupling data, which were given as mean ± SD. Statistical significance between groups was determined by the analysis of variance and Student's *t*-test. $p < 0.05$ was considered to be statistically significant.

Results

Diabetes was confirmed in streptozotocin (STZ)-injected rats by monitoring weight loss and a significant increase in blood glucose levels. Compared to control animals, plasma triglyceride and ALT levels were increased by factors of three and four, respectively, in the diabetic animals, while AST remained unchanged (data not shown). These parameters indicate that the diabetic animals had non-alcoholic fatty liver damage, which is consistent with the STZ model [29]. One month after the onset of the disease, we used *in vivo* spin-trapping techniques with EPR to assess free radical production in the bile of the animals. In spin trapping, short-lived free radical intermediates react with the spin-trapping agent, producing stable free radical adducts that are excreted in the bile. These can then be detected and characterized through their unique signature EPR spectra. Moreover, the fraction of the radicals trapped is proportional to the total amount of the given free radical produced, thereby allowing comparative quantitation [34].

Experiments performed in diabetic rats led to the detection of strong six-line EPR signals of a POBN radical adduct which were reproducibly observed in the bile of rats 2 h after spin trap administration (Fig. 1B). In age- and weight-matched controls, residual signals of POBN radical adducts were recorded (Fig. 1A), confirming increased free radical formation in the diabetic animals. The free radicals trapped were identified through their EPR parameters, $a^{N} = 15.75 \pm 0.06$ G and $a_{\beta}^{H} = 2.77 \pm 0.07$ G, corresponding to those reported previously for the POBN radical adduct of a carbon-centered, lipid-derived radical [32].

One possible candidate for triggering lipid peroxidation is the hydroxyl radical ($^{\bullet}OH$). As the $^{\bullet}OH$ radical adduct of POBN is unstable, a $^{\bullet}OH$ scavenger, dimethyl sulfoxide (DMSO), was used to determine whether $^{\bullet}OH$ radicals were produced. It is well-known that $^{\bullet}OH$ is specifically converted into a methyl radical ($^{\bullet}CH_3$) through its diffusion-limited reaction with DMSO ($k = 7 \times 10^9\ M^{-1}s^{-1}$) [40]. The $^{\bullet}CH_3$ radical and closely related species are then trapped and detected by EPR as POBN-radical adducts. In rat bile, these POBN radical adduct signals increased significantly as early as 30 min after the simultaneous administration of POBN and DMSO in the STZ-treated rats (Fig. 1C). *Ex vivo* studies confirmed the *in vivo* origin of the radical adduct formation. Only a minor background POBN radical adduct signal was noted following addition of POBN (20 mM) and DMSO (10 mM) in collecting tubes containing bile from diabetic rats (Fig. 1D). The same characteristic POBN-lipid radical adduct was detected

in the lipid extracts of kidneys from diabetic animals, but the intensity was only twofold higher than controls (Fig. 1E and F).

Use of ^{13}C-labeled DMSO led to the detection of a twelve-line signal in diabetic, but not control bile (Fig. 2), providing further evidence for the fundamental role of the $^{\bullet}$OH radicals in the diabetic animals. Computer simulation [38] of the EPR spectrum (Fig. 2C–F) confirmed the presence of the POBN/$^{\bullet}$^{13}C-methyl, and possibly closely related species such as POBN/$^{\bullet}$^{13}CH$_2$OH (40) (a^N = 16.02 ± 0.02 G, a_β^H = 2.98 ± 0.14 G, and $a^{13}C$ = 4.59 ± 0.13 G). POBN/$^{\bullet}$L was indicated by a^N =15.72 ± 0.11 G, a_β^H = 2.92 ± 0.11 G [32].

We next investigated in deeper detail the mechanism of free radical production and the possible origin of the $^{\bullet}$OH produced in the progression of STZ-induced diabetes. For this, injections of known metabolic enzyme inhibitors in the diabetic rats were performed before the administration of the spin trap (Fig. 3A). The xanthine oxidase inhibitor allopurinol (100 mg/kg, i.p.) [35] given to rats 24 and 5 h before spin trapping with POBN had no effect on free radical generation in diabetic animals. Likewise, pretreatment with 1-aminobenzotriazle (ABT) (100 mg/kg, i.p.) [33], a suicide substrate of cytochrome P450s, did not not affect the radical generation compared to the untreated diabetic group.

To study the possible role of transition metal ions in the generation of $^{\bullet}$OH, diabetic animals were pretreated with the potent iron chelator Desferal (50 or 200 mg/kg, i.p., 1 h before spin trapping) [34]. We also investigated whether phagocytic activation might be involved in, or related to, free radical production using gadolinium chloride ($GdCl_3$), a phagocytic suppressing agent (10 mg/kg, i.v.), 24 h before the experiments [36]. Neither the iron chelator Desferal nor $GdCl_3$ was found to cause any significant change in radical production in this disease model (Fig. 3A).

In contrast, a dramatic decrease in the formation of free radicals was found in the diabetic animals when the non-specific nitric oxide synthase (NOS) inhibitor aminoguanidine (200 mg/kg, i.p.) was administered 30 min prior to the POBN/DMSO injection [37] (Fig. 3A and B). This effect was even more pronounced when rats were injected with 1400W (15 mg/kg, i.p.), a specific inhibitor of the inducible form of NOS (iNOS) [41], 1 h before spin trap administration (Fig. 3A and B). The inhibiting effect remained for over 2 h (data not shown), and only a residual EPR signal of POBN radical adducts was detected 30 min after injection with POBN/DMSO. To determine if 1400W affected the yield of the lipid and the methyl radicals trapped in the presence of DMSO differently, we performed additional studies with ^{13}C-DMSO and 1400W. As shown in Fig. 3C, the hyperfine structure of the spectrum was not changed from Fig 2B, thus indicating that both methyl and lipid radicals were secondary species derived from the $^{\bullet}$OH reaction with DMSO and lipids, respectively.

The lack of an effect from Desferal revealed that hydroxyl radical production was independent of iron catalysis, suggesting peroxynitrite production since spontaneous peroxynitrite decomposition is a known metal-independent source of hydroxyl radicals. In addition, none of the metabolic inhibitors tested other than the iNOS inhibitors inhibited the free radical formation. This suggests a close relationship between nitric oxide and subsequent $^{\bullet}$OH production. Taken together, these results suggest a significant contribution of iNOS in the mechanism. Nitric oxide synthase have also been demonstrated to be able to produce both $^{\bullet}$NO and $O_2^{\bullet-}$ simultaneously [42] and could thus be the source of peroxynitrite and, consequently, $^{\bullet}$OH. Other possible sources of superoxide, such as the mitochondria, and NADPH oxidases cannot be excluded as well in our model but we have no data to confirm that. To further test the role of iNOS, diabetic rats were injected with L–arginine (100 mg/kg) 30 min before applying POBN. This treatment should diminish $O_2^{\bullet-}$ generation that occurs in the absence of L-arginine and, thus, peroxynitrite production. Indeed, L–arginine pretreatment

consistently prevented lipid radical formation, leaving only a minor background EPR signal of the POBN adduct (Fig. 4).

In addition to these mechanistic studies, time course EPR experiments of bile collected from animals 1, 2 and 3 weeks following STZ injection revealed significantly increased lipid radical production after three weeks of diabetes compared to control animals (Fig. 5). Together with increased formation of free radical intermediates at 3 weeks, iNOS protein expression was considerably augmented in the liver and in the kidney, known target organs for diabetes (Fig. 6A and B). In tissues that are not affected in diabetes such as the lung, iNOS overexpression was not observed (Fig. 6C).

To gather further insight about iNOS expression patterns in the liver of diabetic animals and to further examine the key role of peroxynitrite in the concomitant protein damage, confocal microscopy of *in situ* fixed liver slices obtained from control and diabetic animals was performed. Nitrotyrosine was utilized as a marker of protein modification/oxidation resulting from increased reactive species production. As shown in Fig. 7., increased iNOS immunostaining was apparent in the diabetic liver and was consistently more intense around vessels of pericentral hepatocytes (Fig. 7A and B). Positive nitrotyrosine staining was also observed in the diabetic slices (Fig. 7C and D), and presented considerable colocalization with iNOS (Fig 7E and F). This data suggests that iNOS overexpression led to protein nitration, which is consistent with peroxynitrite formation.

Additional immunohistochemical studies revealed significantly increased 4-hydroxynonenal formation and conjugation to proteins in the liver (Fig. 8A and B) and kidney (Fig. 8C and D) of diabetic animals. 4-Hydroxynonenal is a well characterized aldehyde product of lipid peroxidation which reacts with protein amine groups to produce chemical modification of proteins and enzymes, thus possibly contributing to the complications of diabetes (Fig. 8A and B). In the lung, which is not a target organ, low levels of lipid peroxidation were detected in comparison with controls, which was consistent with the absence of iNOS overexpression in that organ (Fig. 8E and F). Taken together, our results strongly support a mechanism where EPR-detectable radical adducts in diabetic bile and kidney are iNOS-dependent, possibly leading to increased lipid peroxidation and protein modification.

Discussion

Diabetes is known to be a major metabolic disorder in which oxidative stress and free radical production have been implicated through several lines of evidence. Our study suggests a free radical mechanism, where iNOS-mediated hydroxyl radical production plays a significant role in the initiation of lipid peroxidation in STZ-diabetic bile and kidney, which might be contributing to diabetes progression. We have to note here that though streptozotocin-induced diabetes is a very common and intrinsic model of uncontrolled diabetes, it is not an analogue of the human disease. Streptozotocin is a glucose-like molecule with a nitrosourea moiety. Thus, it enters the β-cells through glucose transporters, thereby poisoning them [43].

Here, we have directly demonstrated the production of lipid radicals by EPR spin trapping and established $^{\bullet}$OH as the initiator of the lipid peroxidation through the use of ordinary and isotopically labeled DMSO (Fig. 1, Fig. 2). We have characterized the enzyme involved in the augmentation of radical production using a selection of well-described and reasonably specific metabolic inhibitors (Fig. 3, Fig. 4) to evaluate known alternative sources of reactive intermediates, namely, xanthine oxidase, cytochrome P450s, or phagocytic cell activation [33–36]. Our data clearly demonstrate that none of these enzymes or processes plays a significant role in diabetes-derived oxidative stress in the STZ model. These studies demonstrated iNOS as a major source of $^{\bullet}$OH. Furthermore, through a set of time course

experiments, we detected a close correlation between the levels of free radical production and iNOS protein expression (Fig. 5). We propose that iNOS is likely to mediate peroxynitrite formation and, consequently, •OH production since the process was strongly inhibited by L-arginine, a substrate of this enzyme (Fig. 4). Finally, overexpression of iNOS was localized in the diabetic liver and kidney, as were specific markers of protein chemical modification such as protein-bound 4-hydroxynonenal and nitrotyrosine (Fig. 6–Fig 8). This result specifically reveals oxidative damage to proteins and lipids in the model with the accumulation of oxidized protein end products. Both protein bound to 4-hydroxynonenal and nitrotyrosine staining detected by immunohistochemistry in the liver show considerable colocalization with the sites of maximum iNOS expression as well.

The failure of Desferal to affect •OH production precluded the Fenton reaction as a source of •OH [44]. This potent iron chelator has previously been shown to inhibit metal-dependent Fenton-type reactions [34]. The strong inhibition elicited by both L-arginine and 1400W upon lipid radical formation clearly establishes a connection between iNOS and •OH production. The iNOS inhibitor 1400W was demonstrated to cause irreversible inhibition of the enzyme by inducing extensive chemical modification of the heme site, rendering the enzyme unable to oxygenate L-arginine [45]. The fact that L-arginine abrogated free radical production is consistent with an iNOS-dependent but transition metal-independent route for hydroxyl radical production, which induces lipid peroxidation in the diabetic animals.

Under these circumstances, other nitric oxide synthases have previously been shown to produce •NO and $O_2^{\bullet -}$ simultaneously, leading to peroxynitrite production [42;46;47], which is a transition metal-independent source of •OH [48–52]. Although peroxynitrite homolysis to •OH is expected to be a minor route *in vivo*, such a reaction may acquire significant relevance in hydrophobic environments and initiate lipid peroxidation [53]. Peroxynitrite may further contribute to NOS uncoupling as well, by promoting tetrahydrobiopterin depletion [42;47] and direct enzyme modification [54]. Several other sources, for example, mitochondrial oxidative stress and activation of NADPH oxidases in diabetes may also contribute to superoxide production, which then rapidly reacts with •NO to form the deleterious peroxynitrite. Consistent with an increased production of reactive nitrogen species and, in particular, peroxynitrite, increased nitrotyrosine formation was detected. The hydroxyl radical-driven lipid peroxidation was further characterized through immunohistochemistry using 4-hydroxynonenal protein adducts as a specific marker. The significantly increased staining of the diabetic liver and the significant staining of the diabetic kidney confirmed lipid peroxidation as a consequence of increased free radical production in the disease.

The high correlation of iNOS expression, free radical production, and lipid peroxidation in two diabetic target organs (liver and kidney) and the absence of iNOS in the lung, which was less affected by oxidative damage, support the conclusion that iNOS is a significant source of EPR-detectable products in diabetic bile and kidneys. Our results are further supported by previous studies in the STZ model, where nitric oxide formation was increased during the progression of diabetes as early as three weeks after the onset of the disease in diabetic liver and kidneys, suggesting that augmented nitric oxide synthase activity provoked by the disease [55] leads to the formation of peroxynitrite, which has been implicated in neuropathy or vascular complications [20;56].

It is noteworthy that there is also abundant evidence indicating that iNOS mediates insulin resistance where inflammatory processes are involved [57;58]. For example, the enzyme seems to be markedly expressed in insulin-sensitive organs such as liver, skeletal muscle, and adipose tissue.

In summary, our work demonstrated that •OH radical production arising from peroxynitrite formation as a result of iNOS overexpression may potentially be a primary event which leads to lipid peroxidation in an animal model of streptozotocin-induced diabetes. Detection of *in vivo* free radical generation, the identification of iNOS as a significant free radical source in diabetic bile and kidneys, and the observation of the related lipid and protein damage provide new insight necessary to understand free radical mechanisms behind diabetic complications.

Acknowledgements

The authors thank Dr. David S. Miller and Dr. Kevin Gerrish for valuable advice, Natasha Clayton and Yvette Rebolloso for the outstanding immunohistochemical analysis, Jean B. Corbett for excellent technical assistance, and Dr. Ann Motten and Mary J. Mason for helpful comments made during the preparation of the manuscript. This research was supported by the Intramural Research Program of the NIH, National Institute of Environmental Health Sciences.

Abbreviations

DMSO, dimethyl sulfoxide; EPR, electron paramagnetic resonance; GAPDH, glyceraldehyde-3-phosphate dehydrogenase; iNOS, inducible nitric oxide synthase; POBN, α-(4-pyridyl-1-oxide)-N-tert-butylnitrone; STZ, streptozotocin.

References

1. Wild S, Roglic G, Green A, Sicree R, King H. Global prevalence of diabetes: estimates for the year 2000 and projections for 2030. Diabetes Care 2004;27:1047–1053. [PubMed: 15111519]
2. Kasuga M. Insulin resistance and pancreatic beta cell failure. J Clin Invest 2006;116:1756–1760. [PubMed: 16823472]
3. Centers for Medicare & Medicaid Services (U.S.). Diabetes booklet. Baltimore, Md.: Centers for Medicare & Medicaid Services; 2004.
4. UK Prospective Diabetes Study (UKPDS) Group. Intensive blood-glucose control with sulphonylureas or insulin compared with conventional treatment and risk of complications in patients with type 2 diabetes (UKPDS 33). Lancet 1998;352:837–853. [PubMed: 9742976]
5. The Diabetes Control and Complications Trial/Epidemiology of Diabetes Interventions and Complications Research Group. Retinopathy and nephropathy in patients with type 1 diabetes four years after a trial of intensive therapy. N Engl J Med 2000;342:381–389. [PubMed: 10666428]
6. Basta G, Schmidt AM, De Caterina R. Advanced glycation end products and vascular inflammation: implications for accelerated atherosclerosis in diabetes. Cardiovasc Res 2004;63:582–592. [PubMed: 15306213]
7. Koya D, Jirousek MR, Lin YW, Ishii H, Kuboki K, King GL. Characterization of protein kinase C beta isoform activation on the gene expression of transforming growth factor-beta, extracellular matrix components, and prostanoids in the glomeruli of diabetic rats. J Clin Invest 1997;100:115–126. [PubMed: 9202063]
8. Oates PJ, Mylari BL. Aldose reductase inhibitors: therapeutic implications for diabetic complications. Expert Opin Investig Drugs 1999;8:2095–2119.
9. Ramasamy R, Oates PJ, Schaefer S. Aldose reductase inhibition protects diabetic and nondiabetic rat hearts from ischemic injury. Diabetes 1997;46:292–300. [PubMed: 9000707]
10. Baynes JW. Role of oxidative stress in development of complications in diabetes. Diabetes 1991;40:405–412. [PubMed: 2010041]
11. Dandona P, Thusu K, Cook S, Snyder B, Makowski J, Armstrong D, Nicotera T. Oxidative damage to DNA in diabetes mellitus. Lancet 1996;347:444–445. [PubMed: 8618487]
12. Martin-Gallan P, Carrascosa A, Gussinye M, Dominguez C. Biomarkers of diabetes-associated oxidative stress and antioxidant status in young diabetic patients with or without subclinical complications. Free Radic Biol Med 2003;34:1563–1574. [PubMed: 12788476]

13. Mohamed AK, Bierhaus A, Schiekofer S, Tritschler H, Ziegler R, Nawroth PP. The role of oxidative stress and NF-kappaB activation in late diabetic complications. Biofactors 1999;10:157–167. [PubMed: 10609877]

14. Seghrouchni I, Drai J, Bannier E, Riviere J, Calmard P, Garcia I, Orgiazzi J, Revol A. Oxidative stress parameters in type I, type II and insulin-treated type 2 diabetes mellitus; insulin treatment efficiency. Clin Chim Acta 2002;321:89–96. [PubMed: 12031597]

15. VanderJagt DJ, Harrison JM, Ratliff DM, Hunsaker LA, Vander Jagt DL. Oxidative stress indices in IDDM subjects with and without long-term diabetic complications. Clin Biochem 2001;34:265–270. [PubMed: 11440725]

16. Jay D, Hitomi H, Griendling KK. Oxidative stress and diabetic cardiovascular complications. Free Radic Biol Med 2006;40:183–192. [PubMed: 16413400]

17. Drel VR, Pacher P, Stevens MJ, Obrosova IG. Aldose reductase inhibition counteracts nitrosative stress and poly(ADP-ribose) polymerase activation in diabetic rat kidney and high-glucose-exposed human mesangial cells. Free Radic Biol Med 2006;40:1454–1465. [PubMed: 16631535]

18. Obrosova IG, Pacher P, Szabo C, Zsengeller Z, Hirooka H, Stevens MJ, Yorek MA. Aldose reductase inhibition counteracts oxidative-nitrosative stress and poly(ADP-ribose) polymerase activation in tissue sites for diabetes complications. Diabetes 2005;54:234–242. [PubMed: 15616034]

19. Obrosova IG, Drel VR, Pacher P, Ilnytska O, Wang ZQ, Stevens MJ, Yorek MA. Oxidative-nitrosative stress and poly(ADP-ribose) polymerase (PARP) activation in experimental diabetic neuropathy: the relation is revisited. Diabetes 2005;54:3435–3441. [PubMed: 16306359]

20. Obrosova IG, Mabley JG, Zsengeller Z, Charniauskaya T, Abatan OI, Groves JT, Szabo C. Role for nitrosative stress in diabetic neuropathy: evidence from studies with a peroxynitrite decomposition catalyst. Faseb J 2005;19:401–403. [PubMed: 15611153]

21. Du X, Matsumura T, Edelstein D, Rossetti L, Zsengeller Z, Szabo C, Brownlee M. Inhibition of GAPDH activity by poly(ADP-ribose) polymerase activates three major pathways of hyperglycemic damage in endothelial cells. J Clin Invest 2003;112:1049–1057. [PubMed: 14523042]

22. Brownlee M. The pathobiology of diabetic complications: a unifying mechanism. Diabetes 2005;54:1615–1625. [PubMed: 15919781]

23. Hink U, Li H, Mollnau H, Oelze M, Matheis E, Hartmann M, Skatchkov M, Thaiss F, Stahl RA, Warnholtz A, Meinertz T, Griendling K, Harrison DG, Forstermann U, Munzel T. Mechanisms underlying endothelial dysfunction in diabetes mellitus. Circ Res 2001;88:E14–E22. [PubMed: 11157681]

24. Pieper GM. Acute amelioration of diabetic endothelial dysfunction with a derivative of the nitric oxide synthase cofactor, tetrahydrobiopterin. J Cardiovasc Pharmacol 1997;29:8–15. [PubMed: 9007664]

25. Srinivasan S, Hatley ME, Bolick DT, Palmer LA, Edelstein D, Brownlee M, Hedrick CC. Hyperglycaemia-induced superoxide production decreases eNOS expression via AP-1 activation in aortic endothelial cells. Diabetologia 2004;47:1727–1734. [PubMed: 15490108]

26. Tabatabaie T, Vasquez-Weldon A, Moore DR, Kotake Y. Free radicals and the pathogenesis of type 1 diabetes: beta-cell cytokine-mediated free radical generation via cyclooxygenase-2. Diabetes 2003;52:1994–1999. [PubMed: 12882915]

27. Inoguchi T, Li P, Umeda F, Yu HY, Kakimoto M, Imamura M, Aoki T, Etoh T, Hashimoto T, Naruse M, Sano H, Utsumi H, Nawata H. High glucose level and free fatty acid stimulate reactive oxygen species production through protein kinase C--dependent activation of NAD(P)H oxidase in cultured vascular cells. Diabetes 2000;49:1939–1945. [PubMed: 11078463]

28. Yamada K, Inoue D, Matsumoto S, Utsumi H. In vivo measurement of redox status in streptozotocin-induced diabetic rat using targeted nitroxyl probes. Antioxid Redox Signal 2004;6:605–611. [PubMed: 15130287]

29. Ohno T, Horio F, Tanaka S, Terada M, Namikawa T, Kitoh J. Fatty liver and hyperlipidemia in IDDM (insulin-dependent diabetes mellitus) of streptozotocin-treated shrews. Life Sci 2000;66:125–131. [PubMed: 10666008]

30. Obrosova IG, Fathallah L, Liu E, Nourooz-Zadeh J. Early oxidative stress in the diabetic kidney: effect of DL-alpha-lipoic acid. Free Radic Biol Med 2003;34:186–195. [PubMed: 12521600]

31. Karunanayake EH, Hearse DJ, Mellows G. The synthesis of [14C] streptozotocin and its distribution and excretion in the rat. Biochem J 1974;142:673–683. [PubMed: 4282704]
32. Sato K, Kadiiska MB, Ghio AJ, Corbett J, Fann YC, Holland SM, Thurman RG, Mason RP. In vivo lipid-derived free radical formation by NADPH oxidase in acute lung injury induced by lipopolysaccharide: a model for ARDS. Faseb J 2002;16:1713–1720. [PubMed: 12409313]
33. Mugford CA, Mortillo M, Mico BA, Tarloff JB. 1-Aminobenzotriazole-induced destruction of hepatic and renal cytochromes P450 in male Sprague-Dawley rats. Fundam Appl Toxicol 1992;19:43–49. [PubMed: 1397800]
34. Knecht KT, Mason RP. In vivo spin trapping of xenobiotic free radical metabolites. Arch Biochem Biophys 1993;303:185–194. [PubMed: 8390216]
35. Dikalova AE, Kadiiska MB, Mason RP. An in vivo ESR spin-trapping study: free radical generation in rats from formate intoxication--role of the Fenton reaction. Proc Natl Acad Sci U S A 2001;98:13549–13553. [PubMed: 11717423]
36. Adachi Y, Bradford BU, Gao W, Bojes HK, Thurman RG. Inactivation of Kupffer cells prevents early alcohol-induced liver injury. Hepatology 1994;20:453–460. [PubMed: 8045507]
37. Nakai K, Kadiiska MB, Jiang JJ, Stadler K, Mason RP. Free radical production requires both inducible nitric oxide synthase and xanthine oxidase in LPS-treated skin. Proc Natl Acad Sci U S A 2006;103:4616–4621. [PubMed: 16537416]
38. Duling DR. Simulation of multiple isotropic spin-trap EPR spectra. J Magn Reson B 1994;104:105–110. [PubMed: 8049862]
39. Brito C, Naviliat M, Tiscornia AC, Vuillier F, Gualco G, Dighiero G, Radi R, Cayota AM. Peroxynitrite inhibits T lymphocyte activation and proliferation by promoting impairment of tyrosine phosphorylation and peroxynitrite-driven apoptotic death. J Immunol 1999;162:3356–3366. [PubMed: 10092790]
40. Yue Qian S, Kadiiska MB, Guo Q, Mason RP. A novel protocol to identify and quantify all spin trapped free radicals from in vitro/in vivo interaction of HO(.−) and DMSO: LC/ESR, LC/MS, and dual spin trapping combinations. Free Radic Biol Med 2005;38:125–135. [PubMed: 15589381]
41. Garvey EP, Oplinger JA, Furfine ES, Kiff RJ, Laszlo F, Whittle BJ, Knowles RG. 1400W is a slow, tight binding, and highly selective inhibitor of inducible nitric-oxide synthase in vitro and in vivo. J Biol Chem 1997;272:4959–4963. [PubMed: 9030556]
42. Vasquez-Vivar J, Kalyanaraman B. Generation of superoxide from nitric oxide synthase. FEBS Lett 2000;481:305–306. [PubMed: 11041680]
43. van Zwieten PA. Diabetes and hypertension: experimental models for pharmacological studies. Clin Exp Hypertens 1999;21:1–16. [PubMed: 10052637]
44. Beckman JS, Beckman TW, Chen J, Marshall PA, Freeman BA. Apparent hydroxyl radical production by peroxynitrite: implications for endothelial injury from nitric oxide and superoxide. Proc Natl Acad Sci U S A 1990;87:1620–1624. [PubMed: 2154753]
45. Zhu Y, Nikolic D, Van Breemen RB, Silverman RB. Mechanism of inactivation of inducible nitric oxide synthase by amidines. Irreversible enzyme inactivation without inactivator modification. J Am Chem Soc 2005;127:858–868. [PubMed: 15656623]
46. Andrew PJ, Mayer B. Enzymatic function of nitric oxide synthases. Cardiovasc Res 1999;43:521–531. [PubMed: 10690324]
47. Vasquez-Vivar J, Hogg N, Martasek P, Karoui H, Pritchard KA Jr, Kalyanaraman B. Tetrahydrobiopterin-dependent inhibition of superoxide generation from neuronal nitric oxide synthase. J Biol Chem 1999;274:26736–26742. [PubMed: 10480877]
48. Bonini MG, Augusto O. Carbon dioxide stimulates the production of thiyl, sulfinyl, and disulfide radical anion from thiol oxidation by peroxynitrite. J Biol Chem 2001;276:9749–9754. [PubMed: 11134018]
49. Bonini MG, Radi R, Ferrer-Sueta G, Ferreira AM, Augusto O. Direct EPR detection of the carbonate radical anion produced from peroxynitrite and carbon dioxide. J Biol Chem 1999;274:10802–10806. [PubMed: 10196155]
50. Goldstein S, Czapski G, Lind J, Merenyi G. Effect of *NO on the decomposition of peroxynitrite: reaction of N2O3 with ONOO. Chem Res Toxicol 1999;12:132–136. [PubMed: 10027789]

51. Lymar SV, Khairutdinov RF, Hurst JK. Hydroxyl radical formation by O-O bond homolysis in peroxynitrous acid. Inorg Chem 2003;42:5259–5266. [PubMed: 12924897]
52. Merenyi G, Lind J, Goldstein S, Czapski G. Peroxynitrous acid homolyzes into *OH and *NO2 radicals. Chem Res Toxicol 1998;11:712–713. [PubMed: 9671529]
53. Szabo C, Ischiropoulos H, Radi R. Peroxynitrite: biochemistry, pathophysiology and development of therapeutics. Nat Rev Drug Discov 2007;6:662–680. [PubMed: 17667957]
54. Zou MH, Shi C, Cohen RA. Oxidation of the zinc-thiolate complex and uncoupling of endothelial nitric oxide synthase by peroxynitrite. J Clin Invest 2002;109:817–826. [PubMed: 11901190]
55. Stadler K, Jenei V, von Bolcshazy G, Somogyi A, Jakus J. Increased nitric oxide levels as an early sign of premature aging in diabetes. Free Radic Biol Med 2003;35:1240–1251. [PubMed: 14607523]
56. Szabo C, Mabley JG, Moeller SM, Shimanovich R, Pacher P, Virag L, Soriano FG, Van Duzer JH, Williams W, Salzman AL, Groves JT. Part I: pathogenetic role of peroxynitrite in the development of diabetes and diabetic vascular complications: studies with FP15, a novel potent peroxynitrite decomposition catalyst. Mol Med 2002;8:571–580. [PubMed: 12477967]
57. Fujimoto M, Shimizu N, Kunii K, Martyn JA, Ueki K, Kaneki M. A role for iNOS in fasting hyperglycemia and impaired insulin signaling in the liver of obese diabetic mice. Diabetes 2005;54:1340–1348. [PubMed: 15855318]
58. Yuan M, Konstantopoulos N, Lee J, Hansen L, Li ZW, Karin M, Shoelson SE. Reversal of obesity- and diet-induced insulin resistance with salicylates or targeted disruption of Ikkbeta. Science 2001;293:1673–1677. [PubMed: 11533494]

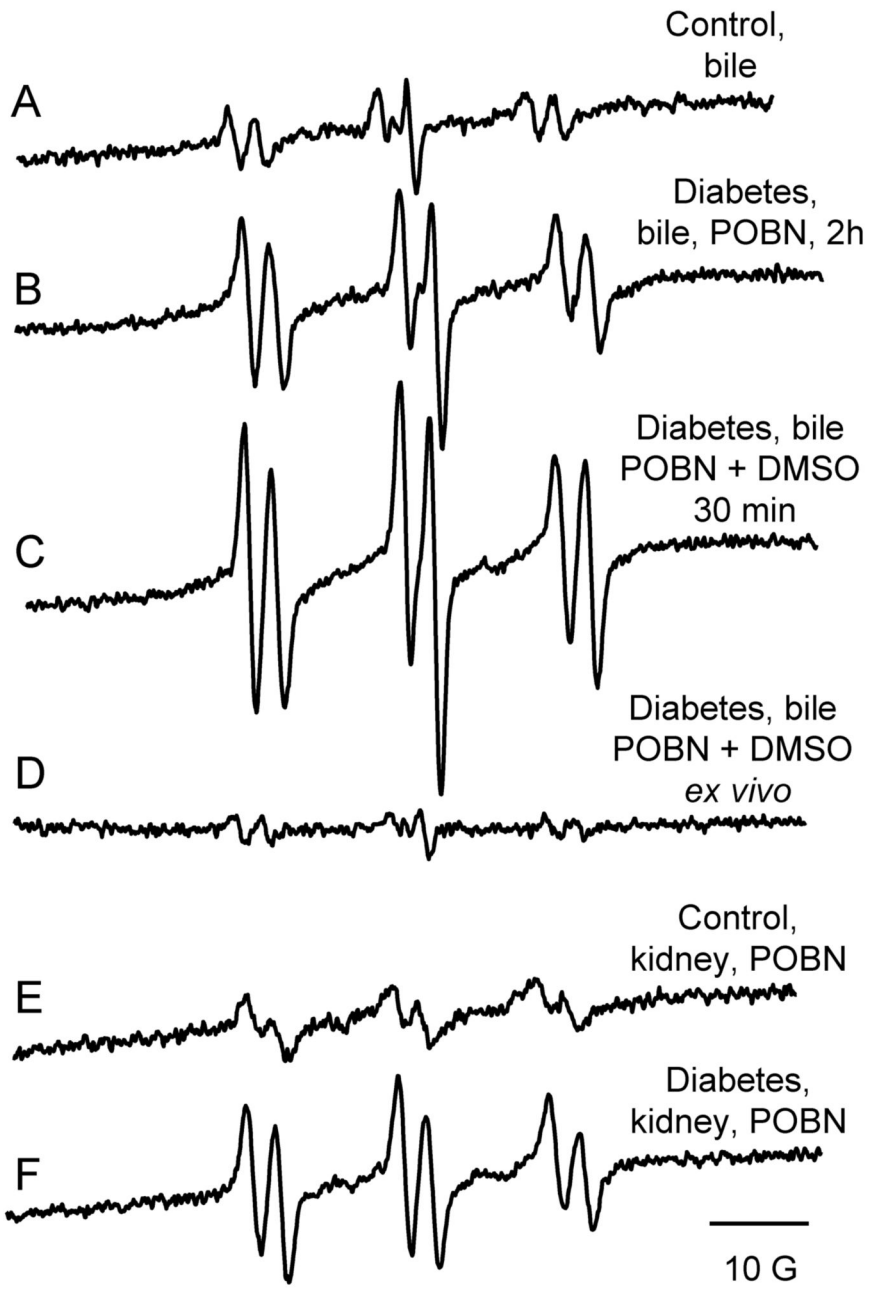

Fig. 1.

Free radical production in STZ-induced diabetes one month after the onset of disease. Representative EPR spectra of POBN radical adducts detected in bile of control (A) or diabetic (B) rats 2 h after POBN injection or in diabetic rats (C) 30 min after the administration of the spin trap POBN (1 g/kg) and DMSO (1 ml/kg). No free radical production was detected if POBN and DMSO were not administered *in vivo* (D). Representative EPR spectra of POBN radical adducts detected in the lipid extracts of the kidney of control (E) and diabetic animals (F). Spectra are representative of at least six independent experiments.

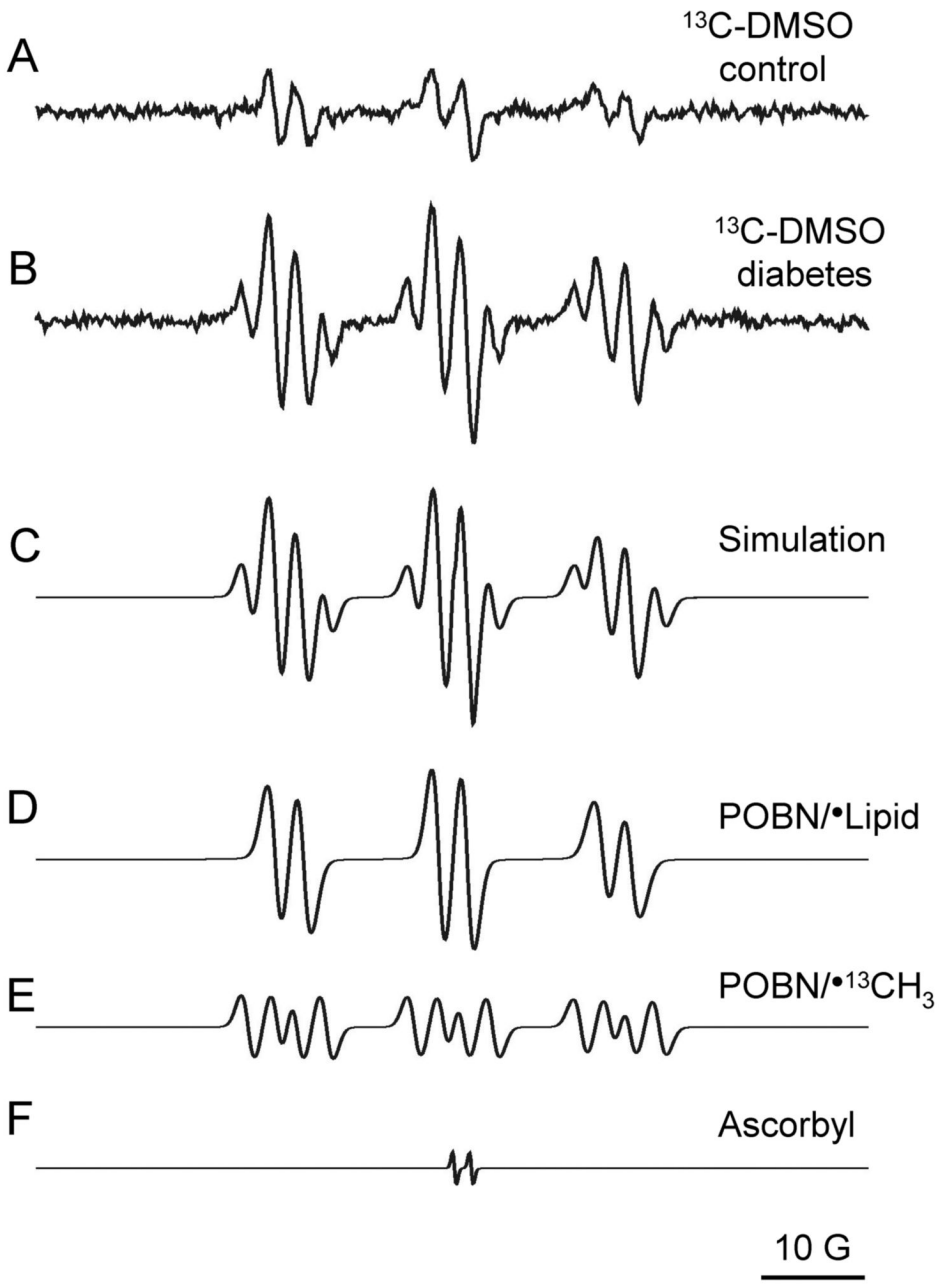

Fig. 2.

Representative EPR spectra of rat bile obtained 30 min after injection of ^{13}C-labeled DMSO (1 ml/kg) and POBN (1 g/kg). Spectrum of untreated control bile (A) showed no extra hyperfine splitting while diabetic bile (B) showed a twelve-line spectrum characteristic of •OH radical production. Composite computer simulation of the spectra (C) allowed us to further characterize and confirm the identities of the radical species being trapped (D–E) and a negligible background from the ascorbate semidione radical (F).

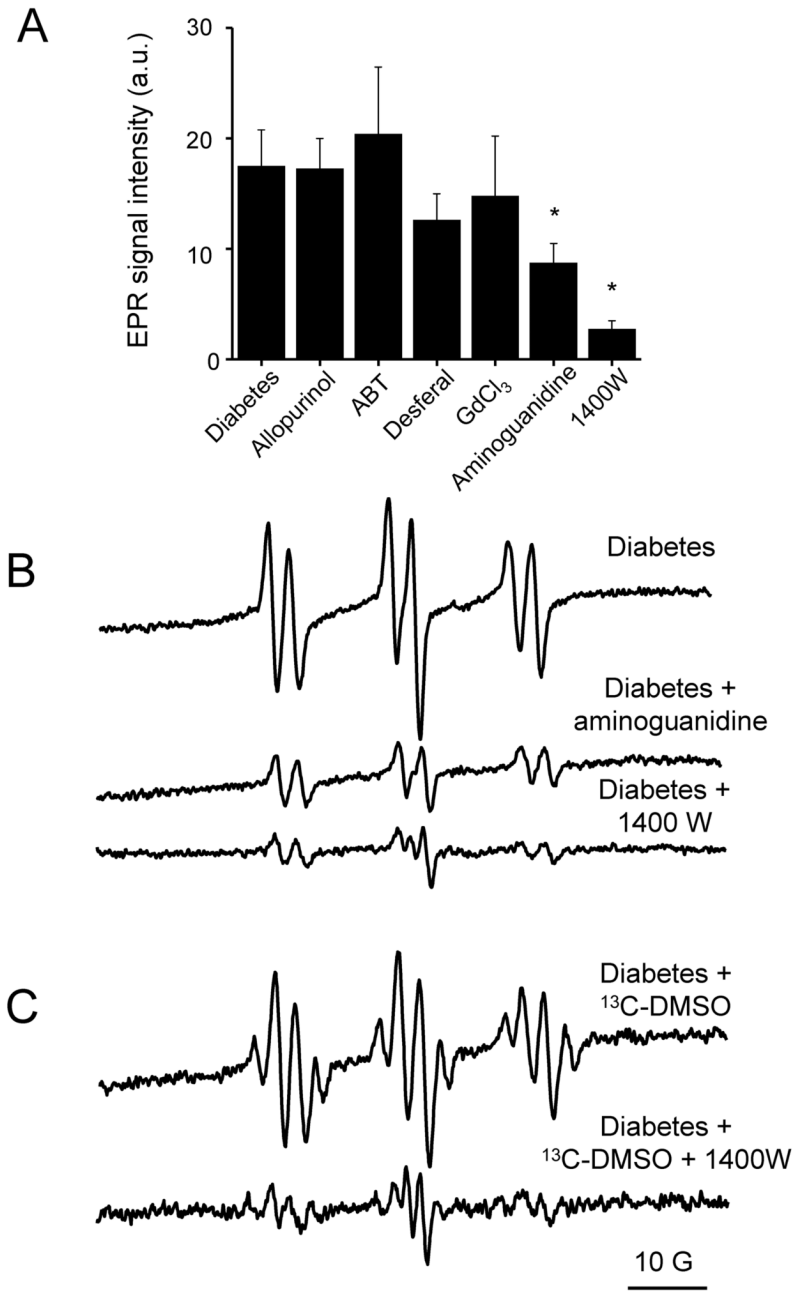

Fig. 3.

Effect of different enzymatic inhibitors on free radical production in diabetic animals. (A) Comparative quantitation of the effects of different inhibitors and treatments on the detectable POBN radical adduct levels detected in diabetic rat bile one month after the onset of the disease. Samples were collected 30 minutes after POBN (1 g/kg, i.p.) and DMSO (1 ml/kg) administration. (B) Representative EPR spectra of POBN radical adducts detected in the diabetic rat bile or in the bile of diabetic rats pretreated with aminoguanidine and 1400W. Spectra are representative of at least six independent experiments. (C) Effect of the iNOS inhibitor 1400W on the ratio of free radical species generated in STZ-induced diabetes. Representative EPR spectra of POBN radical adducts were detected in the bile. Spectra show

bile from an untreated diabetic rat and from a diabetic rat pretreated with 1400W. Spectra are representative of three independent experiments.

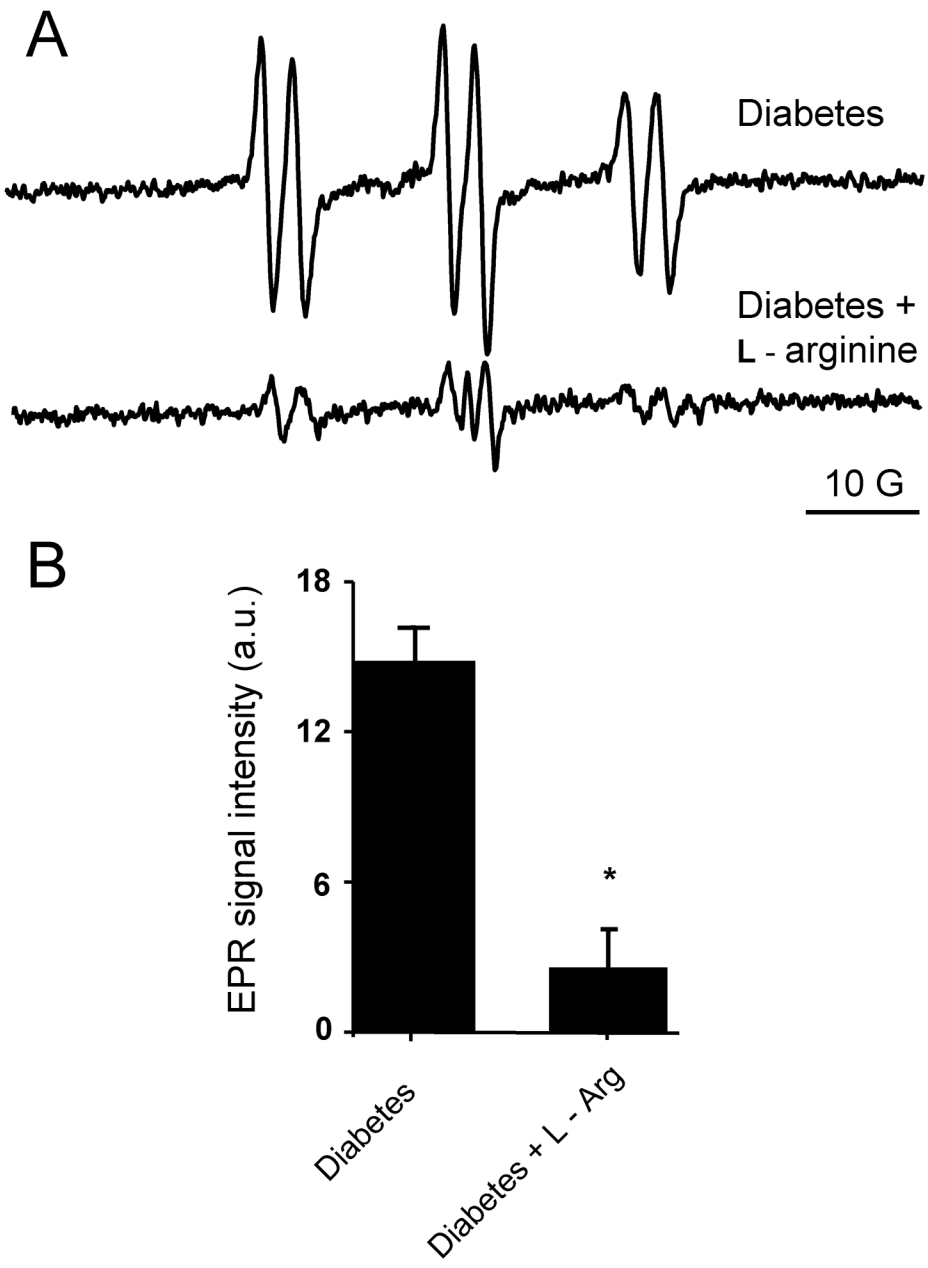

Fig. 4.

Effect of L-arginine pretreatment on free radical generation in diabetic animals. (A) L-arginine administration (100 mg/kg) reduced the detectable free radical level to the background signal. Spectra show bile from an untreated diabetic rat and from a diabetic rat pretreated with L-arginine. Spectra are representative of three independent experiments. (B) Bar values represent mean ± SE of the intensity of the first peak on the spectra derived from the same experiments. * $p < 0.05$ vs. untreated diabetic animals.

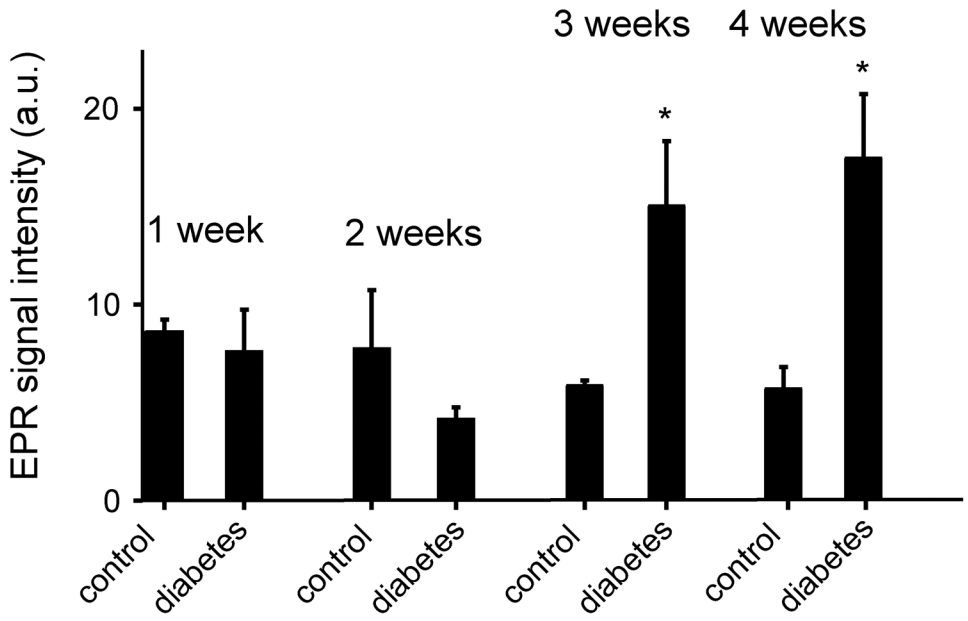

Fig. 5.

Time course study of lipid radical adduct production measured by EPR spectroscopy. POBN/lipid radical adducts were determined in the bile of diabetic and age-matched control rats one, two, three and four weeks after the onset of the disease. Each experiment was repeated in triplicate. * $p < 0.05$ vs. control.

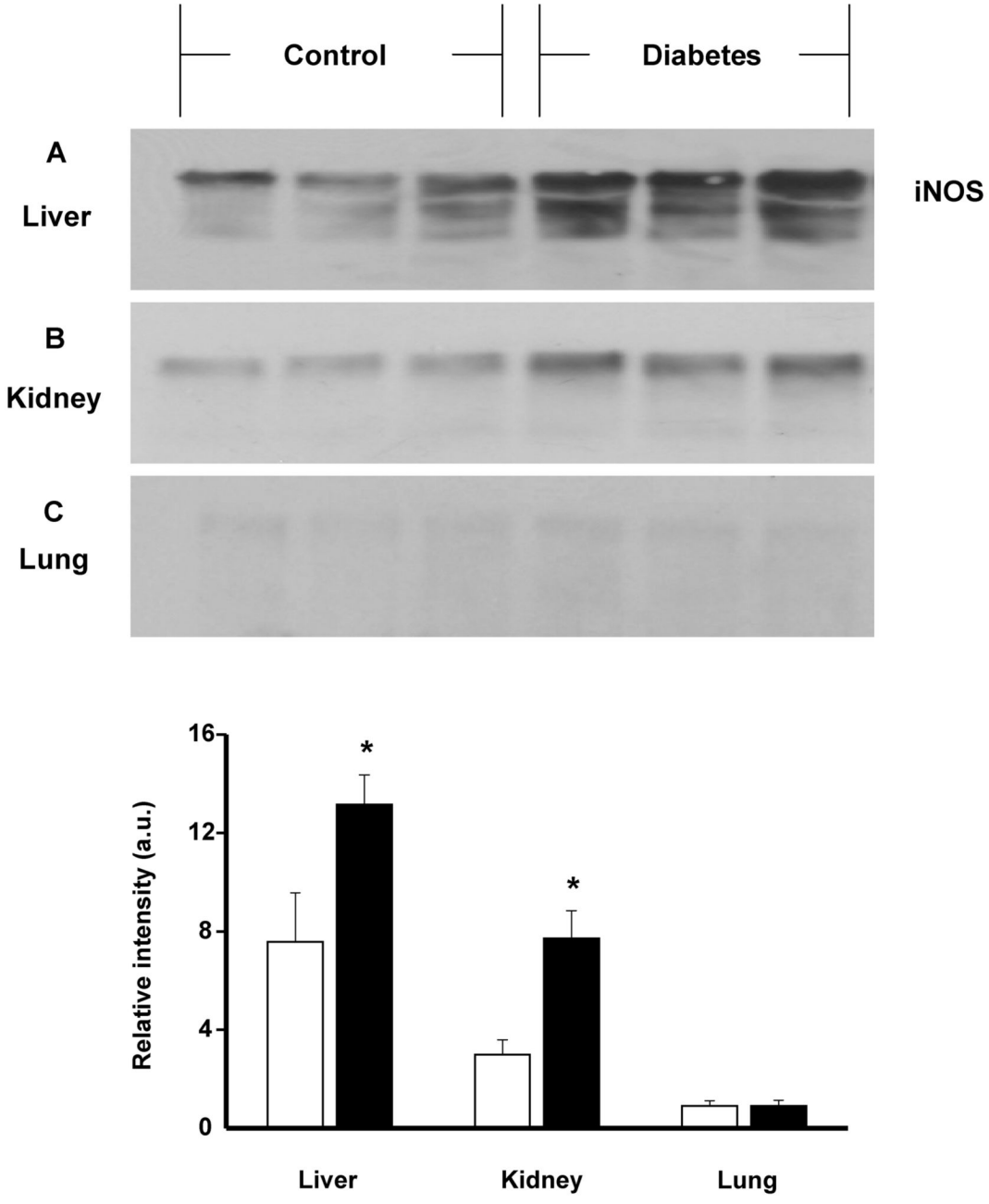

Fig. 6.

Western blot analysis of iNOS protein expression in rat liver (A), kidney (B) and lung (C) tissues after one month of diabetes. Data are representative of three independent experiments. Graph shows the statistics between control (white bar) and diabetic (black bar) groups. * p< . 05.

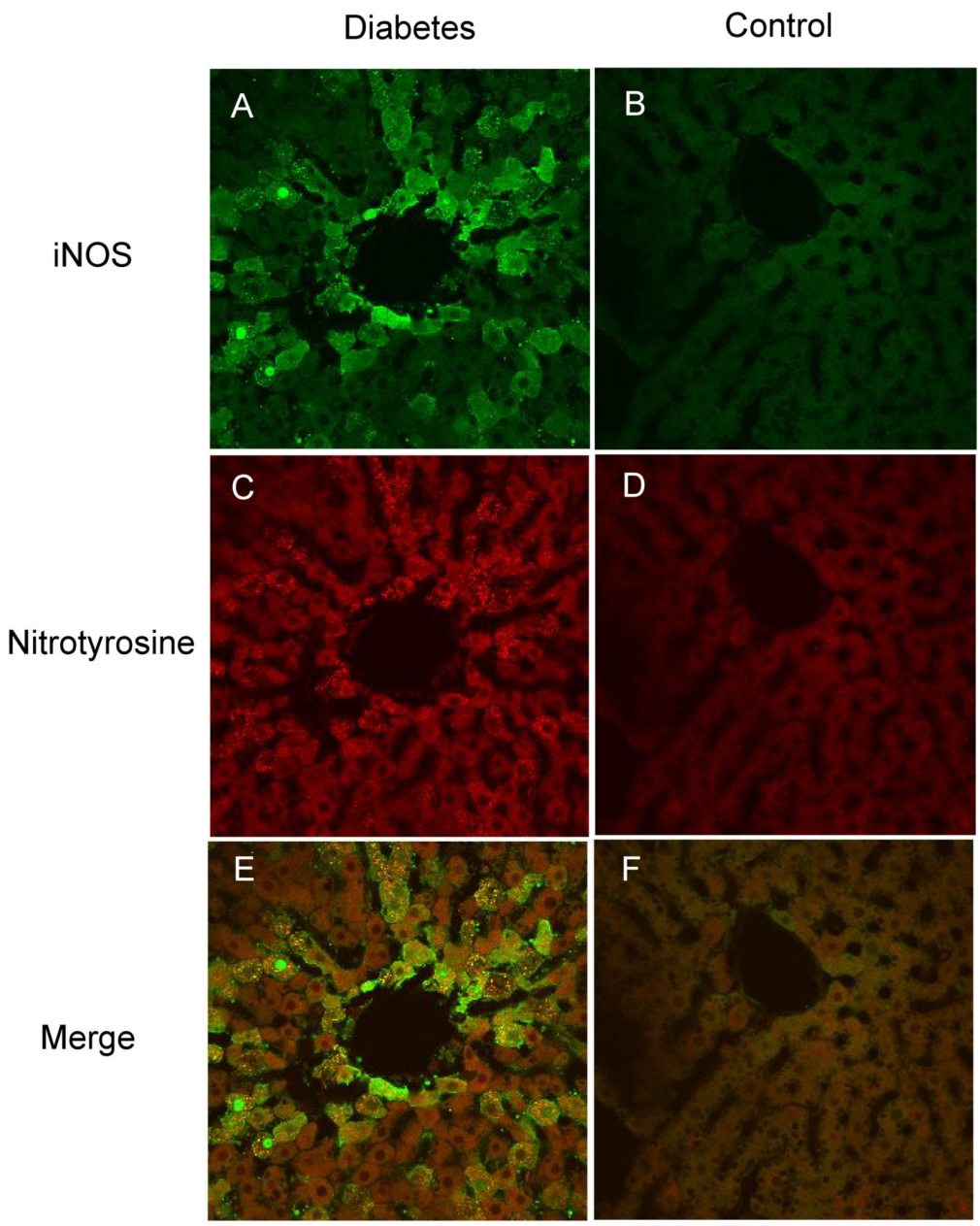

Fig. 7.

Immunofluorescence detection and colocalization of iNOS and nitrotyrosine in rat liver tissues using confocal microscopy. (A) Significant iNOS staining was observed in diabetic rat liver (green labeling). (B) Liver slices from control animals show little iNOS staining. (C) Positive nitrotyrosine staining was detected in the diabetic samples (red labeling). (D) Control liver slices showed negligible staining for nitrotyrosine. (E) and (F) Colocalization of the site of iNOS expression and nitrotyrosine formation. Images are representative of four independent experiments.

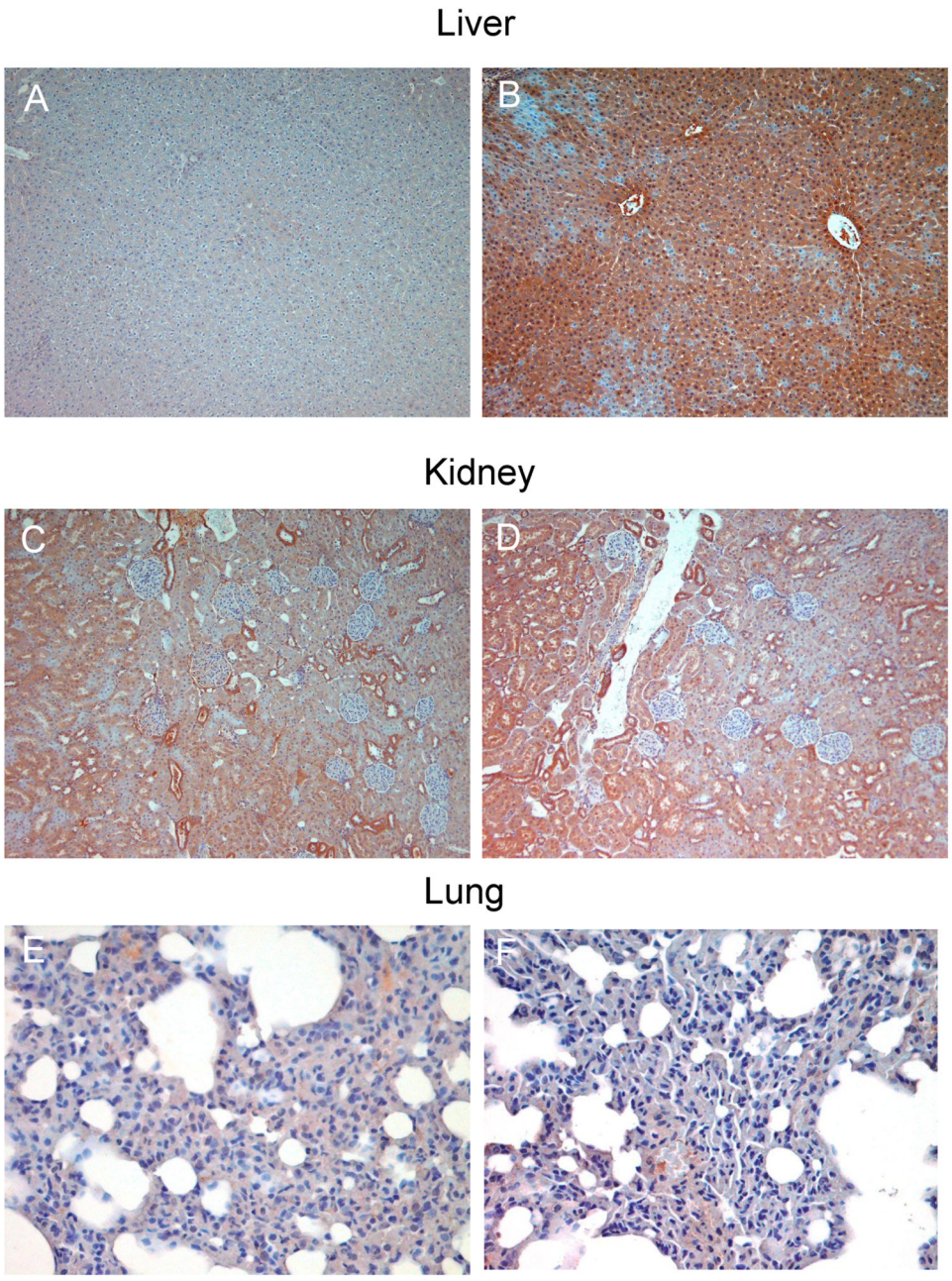

Fig. 8.

Immunohistochemical detection of 4-hydroxynonenal in the diabetic liver, kidney and lung. (A) Control liver samples showed minimal staining; meanwhile, (B) strong positive staining was observed in the diabetic liver. (C) 4-hydroxynonenal detection in control and (D) diabetic kidney – the staining was more pronounced around the tubuli in the diabetic kidney. (E) and (F): control and diabetic lung samples showed no significant difference in 4-hydroxynonenal staining. Images are representative of three independent experiments.